

# GaAs-based long-wavelength InAs bilayer quantum dots grown by molecular beam epitaxy\*

Zhu Yan(朱岩)<sup>†</sup>, Li Mifeng(李密锋), He Jifang(贺继方), Yu Ying(喻颖), Ni Haiqiao(倪海桥), Xu Yingqiang(徐应强), Wang Juan(王娟), He Zhenhong(贺振宏), and Niu Zhichuan(牛智川)

State Key Laboratory for Superlattices and Microstructures, Institute of Semiconductors, Chinese Academy of Sciences, Beijing 100083, China

**Abstract:** Molecular beam epitaxy growth of a bilayer stacked InAs/GaAs quantum dot structure on a pure GaAs matrix has been systemically investigated. The influence of growth temperature and the InAs deposition of both layers on the optical properties and morphologies of the bilayer quantum dot (BQD) structures is discussed. By optimizing the growth parameters, InAs BQD emission at 1.436  $\mu\text{m}$  at room temperature with a narrower FWHM of 27 meV was demonstrated. The density of QDs in the second layer is around  $9 \times 10^9$  to  $1.4 \times 10^{10} \text{ cm}^{-2}$ . The BQD structure provides a useful way to extend the emission wavelength of GaAs-based material for quantum functional devices.

**Key words:** InAs bilayer quantum dots; molecular beam epitaxy; long wavelength; photoluminescence

**DOI:** 10.1088/1674-4926/32/8/083001

**PACC:** 6855; 7855E

**EEACC:** 2520D; 2530C

## 1. Introduction

Over the last few years, 1.31  $\mu\text{m}$  to 1.55  $\mu\text{m}$  GaAs based InAs quantum dot (QD) lasers have attracted much attention as they have shown excellent performance indicators, such as stable temperature characteristics<sup>[1]</sup>, low threshold current densities<sup>[2]</sup> and being compatible with the AlGaAs/GaAs distributed Bragg reflector<sup>[3]</sup>. 1.3  $\mu\text{m}$  InAs/GaAs QD lasers, including high performance vertical cavity surface-emitting lasers, have already been demonstrated<sup>[4–6]</sup>. Nowadays, research on the subject has been focused on the 1.5  $\mu\text{m}$  range<sup>[7]</sup>. Both dilute-nitride quantum well (QW) lasers using GaInNAs(Sb) materials and lasers based on the concept of growth of a metamorphic InGaAs buffer on GaAs substrate can be realized in this wavelength range<sup>[8, 9]</sup>. However, several problems still need to be overcome for both, such as a large threshold current density and the complicated device growth.

Recently, a new InAs bilayer QD (BQD) structure enables us to grow InAs/GaAs QDs with only GaAs in the barrier, emitting up to 1.5  $\mu\text{m}$  at room temperature<sup>[10]</sup>. This structure consists of two closely spaced QD layers separated by a thin GaAs spacer layer. If the thickness of the spacer layer is  $\leq 20 \text{ nm}$ <sup>[11, 12]</sup>, the strain field generated by the first (seed) layer will extend through the spacer layer<sup>[11, 13]</sup>, which provides nucleation sites for the second layer and the QD density of the second layer is fixed. A large red-shift of QD emission can be achieved by growing the second layer at a low substrate temperature due to a combination of increased aspect ratio, reduced In/Ga intermixing and strain relaxation<sup>[3, 10]</sup>. In this paper, we investigate the influence of growth temperature and InAs deposition of both the two layers on the optical properties and morphologies on the BQD structures.

## 2. Experimental details

All samples used in this study were grown on  $n^+$  GaAs (100) substrate by a solid source Veeco Mod Gen II molecular beam epitaxy (MBE) system equipped with reflection high-energy electron diffraction (RHEED) for *in situ* monitoring of the growth process, in particular, measuring the critical thickness for QD formation ( $\theta_{\text{crit}}$ ). After removing the oxide, a 300 nm GaAs buffer was grown at 600 °C. BQDs were formed by depositing two InAs QD layers separated by a 10 nm GaAs spacer layer. The InAs deposition rate for both layers was 0.02 ML/s. After deposition,  $\theta_1$  ML InAs at  $T_1$ , the GaAs spacer layer was deposited. The substrate temperature was then changed to  $T_2$  for the growth of the second InAs QD layer with an InAs thickness of  $\theta_2$  ML. In order to further extend the PL emission wavelength, the second layer was capped by a 4 nm  $\text{In}_{0.2}\text{Ga}_{0.8}\text{As}$  layer at the same temperature  $T_2$ . To analyze morphologies, another BQD without the cap layer was grown on top. A schematic diagram of a complete structure is shown in Fig. 1. The morphologies of the QDs in the top layer were evaluated by a nanoscope IIIa atomic force microscope (AFM). PL measurements were taken at room temperature (RT) for all examples with a Fourier transform infrared spectrometer operating with a cooled Ge detector. A Tecnai F20 field emission gun transmission electron microscope (FEG-TEM) was used to evaluate the microstructure and crystal quality of the epitaxial layers. The growth conditions of all samples are listed in Table 1.

## 3. Results and discussion

The dark field TEM image of a BQD is shown in Fig. 2,

\* Project supported by the National Natural Science Foundation of China (Nos. 10734060, 90921015) and the National Basic Research Program of China (Nos. 2007CB936304, 2010CB327601).

<sup>†</sup> Corresponding author. Email: zhuyan09@semi.ac.cn

Received 28 February 2011, revised manuscript received 22 March 2011

© 2011 Chinese Institute of Electronics

Table 1. Growth conditions of samples A1 to C2. Here  $\theta_1$  and  $\theta_2$  are the deposition amounts of In in the two QD layers.  $T_1$  is the growth temperature of the first layer of QDs;  $T_2$  is the growth temperature of the second layer of QDs and the cap layer.

Sample number	InAs deposition amount (ML)		Growth temperature (°C)	
	$\theta_1$	$\theta_2$	$T_1$	$T_2$
A1	2.3	2.3	550	550
A2	2.3	2.8	550	550
A3	2.3	3.2	550	550
A4	2.3	3.6	550	550
B1	2.8	2.8	550	550
C1	2.3	3.2	550	520
C2	2.3	3.2	550	480

InAs QDs $\theta_2$ ML
GaAs 10 nm
InAs QDs $\theta_1$ ML
GaAs 40 nm
In <sub>0.2</sub> Ga <sub>0.8</sub> As 4 nm
InAs QDs $\theta_2$ ML
GaAs 10 nm
InAs QDs $\theta_1$ ML
GaAs buffer 300 nm
n <sup>+</sup> GaAs (100)

Fig. 1. Schematic of InAs BQDs grown on GaAs substrate.

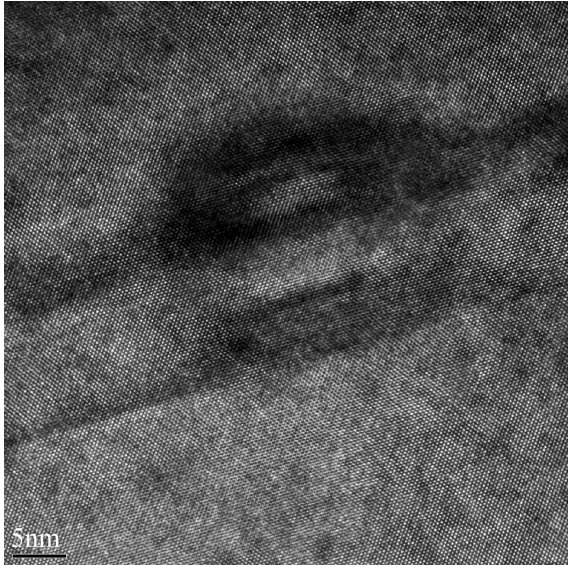


Fig. 2. Cross-sectional dark field TEM image of the BQDs.

which clearly displays the vertical alignment of two layers of QDs. The dot size in the second layer is much larger than that in the first layer and it is believed to be one of the main reasons that the emission wavelength is extended in such structure<sup>[7]</sup>. The material is of high quality as no dislocations can be found in the image and it can be further proved by RTPL tests of the sample.

In Fig. 3, we present the RTPL spectra of BQDs with different InAs deposition amounts  $\theta_2$  in the second layer and a

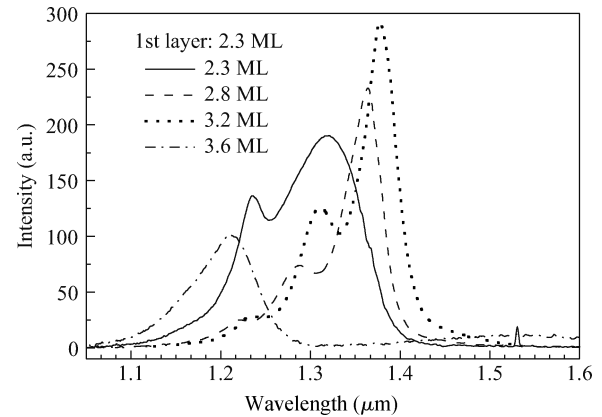


Fig. 3. RTPL spectra of BQDs with different InAs thicknesses  $\theta_2$  in the second layer and a fixed thickness of  $\theta_1 = 2.3$  ML in the first layer.

fixed thickness of 2.3 ML in the first layer for samples A1 to A4. Different InAs deposition amounts in the second layer have a great influence on the optical properties of BQDs. As to A1 to A3, when  $\theta_2$  changes from 2.3 ML to 3.2 ML, the emission wavelength red-shifts with the increase of InAs deposition amounts, which is similar to the situation in the single-layer InAs QDs<sup>[14]</sup>. The emission wavelength reaches a maximum when  $\theta_2$  is up to 3.2 ML. We realized that this red-shift is due to an increased dot size. In addition, the PL full width half maximum (FWHM) decreases as a result of the improved dot size uniformity<sup>[14]</sup>. However, a remarkable blue-shift is observed for A4 as  $\theta_2$  is up to 3.6 ML, accompanied by a reduction of PL intensity and the increase of FWHM. An AFM test shows that QD density of A4 reduced sharply compared to A1 to A3 and some very large dots form. These large QDs are believed to have no contribution to PL emission<sup>[7]</sup>. However, the formation of these large islands brings more crystal defects and/or dislocations. The bigger the QDs' volume becomes, the more defects and/or dislocations they may involve, because they are growing much faster than the smaller ones<sup>[15]</sup>. As the total amount of InAs deposited in the second layer is fixed, the formation of these large islands may reduce the size of QDs around them. Thus, the QD's uniformity in size is reduced and is reflected in the increase of FWHM in A4.

When fixing the InAs thickness of  $\theta_2 = 2.8$  ML in the second layer, sample A2 has an InAs deposition of  $\theta_1 = 2.3$  ML in the first layer and  $\theta_1$  equals 2.8 ML for B1. Figure 4 shows the RTPL spectra of the two samples. No distinct differences of PL

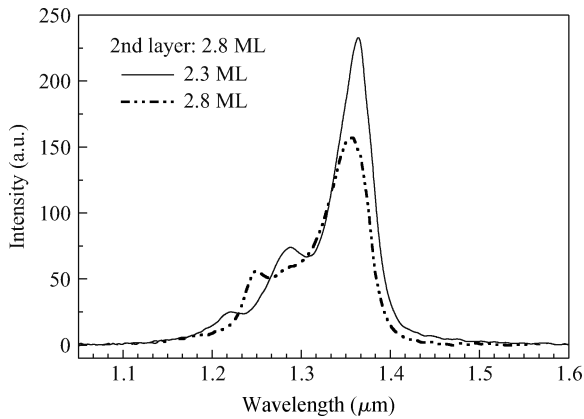


Fig. 4. RTPL spectra of BQDs with different InAs thicknesses  $\theta_1$  in the first layer and a fixed thickness of  $\theta_2 = 2.8$  ML in the second layer.

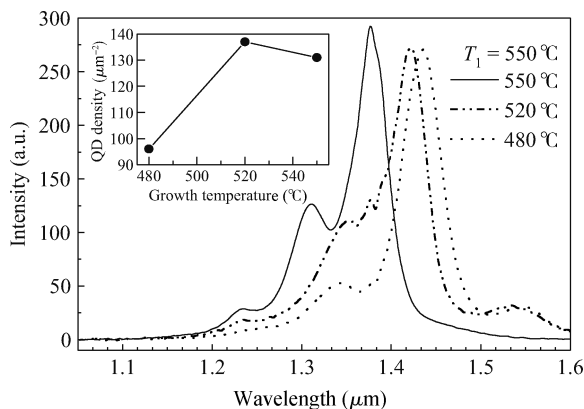


Fig. 5. RTPL spectra of BQDs with different growth temperatures  $T_2$  for the second layer and a fixed growth temperature  $T_1 = 550$  °C for the growth of the first layer and changes of QD densities in the second layer with growth temperature  $T_2$  (inset).

emission wavelength have been found as  $\theta_1$  changes. This may be because the emission is mainly from the second layer. The first layer just provides nucleation sites for the second layer. The comparison of QD densities in the second layer of sample A3 to C1 confirms this conclusion. As shown in the inset of Fig. 5, when  $T_2$  changes from 550 to 520 °C, the QD density in the second layer changes little. However, the reduction of  $T_2$  from 550 to 520 °C would be expected to lead an increase of QD density by a factor of around 4<sup>[16]</sup>. It demonstrates that the strain field generated by the first layer is strong enough to make QDs nucleate only on the top of the existing dots, regardless of the reduction of the diffusion length of In atoms<sup>[10]</sup>.

Figure 5 shows the RTPL spectra of BQDs with different growth temperatures  $T_2$  for the second layer and a fixed growth temperature  $T_1 = 550$  °C for the growth of the first layer. Both the growth and capping temperature for sample A3 is 550 °C. A reduction of  $\theta_{\text{crit}}$  for the second layer compared to the first one (from 2.0 ML to 1.4 ML) is observed through RHEED, which indicates that QDs in the second layer have a bigger volume<sup>[10, 17]</sup>. It may be expected that the QDs in the second layer would be more strain-relaxed<sup>[10]</sup>. This, together with the increased volume of QDs in the second layer<sup>[10]</sup>, should re-

sult in a red-shift of emission wavelength. But the PL emission of sample A3 is not as long as expected. As far as we know, this is because the strain relaxation induces an enhancement of In/Ga intermixing during the capping of the QDs in the second layer<sup>[18, 19]</sup>, which compensates the expected red-shift. In the study of single-layer QDs, low temperature capping was widely used to reduce In/Ga intermixing<sup>[20]</sup>. Here, sample C1 was prepared to make a comparison. It was identical to A3 except that  $T_2$  was reduced to 520 °C for the growth and capping of the second layer. The RTPL spectra of sample C1 is remarkably different from that of A3. The emission wavelength is red-shifted by 45.3 nm, to 1421.8 nm at room temperature. When we further reduce  $T_2$  to 480 °C, an additional red-shift of 14.6 nm is observed in sample C2. The RTPL emission wavelength reaches 1436.4 nm and the FWHM is reduced to 27 meV. Furthermore, we realize that although both the growth and capping at low temperature contribute to red-shift, they have different physical origins<sup>[10]</sup>. The low temperature growth tends to increase the aspect ratio and the low temperature capping contributes to reducing In/Ga intermixing. The reduction of QD density in C2 is due to the increase of QD volume in the second layer, since the total In deposition amount is fixed. The larger dots in the second layer induce the red-shift<sup>[21]</sup>.

## 4. Conclusion

To conclude, we have investigated the MBE growth of InAs BQDs embedded in a pure GaAs matrix on GaAs substrate. By optimizing the InAs deposition amount for the first and second layer and the growth and capping temperature for the second layer, InAs BQD emission at 1.436  $\mu\text{m}$  at room temperature with a narrow FWHM of 27 meV was demonstrated. The density of QDs in the second layer is around  $9 \times 10^9$  to  $1.4 \times 10^{10} \text{ cm}^{-2}$ . Strong PL intensity and narrow FWHM indicate that BQDs are of good quality. The experimental results show that the BQD structures have great potential in the fabrication of GaAs based long wavelength devices.

## References

- [1] Shechkin O B, Ahn J, Deppe D G. High temperature performance of self-organised quantum dot laser with stacked p-doped active region. *Electron Lett*, 2002, 38: 712
- [2] Liu G T, Stintz A, Li H, et al. Extremely low room-temperature threshold current density diode lasers using InAs dots in  $\text{In}_{0.15}\text{Ga}_{0.85}\text{As}$  quantum well. *Electron Lett*, 1999, 35: 1163
- [3] Wang P F, Xiong Y H, Wang H L, et al. GaAs-based metamorphic long-wavelength InAs quantum dots grown by molecular beam epitaxy. *Chin Phys Lett*, 2009, 26: 067801
- [4] Huffaker D L, Park G, Zou Z, et al. 1.3  $\mu\text{m}$  room-temperature GaAs-based quantum-dot laser. *Appl Phys Lett*, 1998, 73: 2564
- [5] Ledentsov N N. Long-wavelength quantum-dot lasers on GaAs substrates: from media to device concepts. *IEEE J Sel Topics Quantum Electron*, 2002, 8: 1015
- [6] Imberg D, Ledentsov N N, Lott J A. Theme article-quantum-dot vertical-cavity surface-emitting lasers. *MRS Bulletin*, 2002, 27: 531
- [7] Li L H, Rossetti M, Patriarcho G, et al. Growth of InAs bilayer quantum dots for long-wavelength laser emission on GaAs. *J Cryst Growth*, 2007, 301: 959

- [8] Bank S R, Wistey M A, Goddard L L, et al. High-performance 1.5  $\mu\text{m}$  GaInNAsSb lasers grown on GaAs. *Electron Lett*, 2004, 40: 1186
- [9] Ledentsov N N, Kovsh A R, Zhukov A E, et al. High performance quantum dot lasers on GaAs substrates operating in 1.5  $\mu\text{m}$  range. *Electron Lett*, 2003, 39: 1126
- [10] Ru E C L, Howe P, Jones T S, et al. Strain-engineered InAs/GaAs quantum dots for long-wavelength emission. *Phys Rev B*, 2003, 67: 165303
- [11] Xie Q, Madhukar A, Chen P, et al. Vertically self-organized InAs quantum box islands on GaAs (100). *Phys Rev Lett*, 1995, 75: 2542
- [12] Mukhametzanov I, Heitz R, Zeng J, et al. Independent manipulation of density and size of stress-driven self-assembled quantum dots. *Appl Phys Lett*, 1998, 73: 1841
- [13] Tersoff J, Teichert C, Lagally M G. Self-organization in growth of quantum dot superlattices. *Phys Rev Lett*, 1996, 76: 1675
- [14] Chu L, Arzberger M, Böhm G, et al. Influence of growth conditions on the photoluminescence of self-assembled InAs/GaAs quantum dots. *J Appl Phys*, 1999, 85: 2355
- [15] Drucker J. Coherent islands and microstructural evolution. *Phys Rev B*, 1993, 48: 18203
- [16] Joyce P B, Krzyzewski T J, Bell G R, et al. Composition of InAs quantum dots on GaAs (001): direct evidence for (In,Ga)As alloying. *Phys Rev B*, 1998, 58: R15981
- [17] Howe P, Ru E C L, Clarke E, et al. Competition between strain-induced and temperature-controlled nucleation of InAs/GaAs quantum dots. *J Appl Phys*, 2004, 95: 2998
- [18] Joyce P B, Ru E C L, Krzyzewski T J, et al. Optical properties of bilayer InAs/GaAs quantum dot structures: influence of strain and surface morphology. *Phys Rev B*, 2002, 66: 075316
- [19] Lipinski M O, Schuler H, Schmidt O G, et al. Strain-induced material intermixing of InAs quantum dots in GaAs. *Appl Phys Lett*, 2000, 77: 1789
- [20] Schmidt O G, Kiravittaya S, Nakamura Y, et al. Self-assembled semiconductor nanostructures: climbing up the ladder of order. *Surf Sci*, 2002, 514: 10
- [21] Zinoni C, Alloying B, Monat C, et al. Time-resolved and anti-bunching experiments on single quantum dots at 1300 nm. *Appl Phys Lett*, 2006, 88: 131102